Int. J. Heat Mass Transfer. Vol. 32, No. 7, pp. 1289–1298, 1989
Printed in Great Britain

0017–9310/89 $3.00+0.00

A numerical analysis of Stefan problems for generalized multi-dimensional phase-change structures using the enthalpy transforming model

YIDING CAO and AMIR FAGHRI
Department of Mechanical Systems Engineering, Wright State University, Dayton, OH 45435, U.S.A.

and

WON SOON CHANG
Wright Research and Development Center, Wright-Patterson Air Force Base, OH 45433, U.S.A.

(*Received* 25 *July* 1988 *and in final form* 15 *December* 1988)

Abstract—An enthalpy transforming scheme is proposed to convert the energy equation into a non-linear equation with the enthalpy, E, being the single dependent variable. The existing control-volume finite-difference approach is modified so it can be applied to the numerical performance of Stefan problems. The model is tested by applying it to a three-dimensional freezing problem. The numerical results are in agreement with those existing in the literature. The model and its algorithm are further applied to a three-dimensional moving heat source problem showing that the methodology is capable of handling complicated phase-change problems with fixed grids.

INTRODUCTION

HEAT FLOW and diffusion with melting and solidification are of great importance in many industrial applications. Examples are casting, welding, thermal energy storage units, heat pipe start-up from the frozen state, etc. The last two operations were the major motivation for the present study. Phase-change processes may produce solid and liquid phase regions which have extremely complex appearances. Also, it is not possible to predict a priori what the phase-change front evolving in time will look like. Therefore, exact analytical solutions for these types of non-linear problems are available only for some simplified and idealized systems. Numerical methods appear to be the only practical method for handling the general melting and freezing problems providing that one can successfully trace the moving interface.

The numerical methods used to solve phase-change problems may be divided into two main groups. The first group is called strong numerical solutions. The focus here is on applying finite-difference and finite-element techniques to the strong formulation of the process, locating fronts and finding temperature distributions at each time step or employing a transformed coordinate system to immobilize the moving interfaces [1, 2]. These methods are applicable to those processes involving one or two phases in one space dimension which, with the use of complicated schemes, are being applied to two-dimensional cases as well.

The second group is called weak numerical solutions [3–8]. These methods allow us to avoid paying explicit attention to the nature of the phase-change front. They appear to have great flexibility and are easily extended to multi-dimensional problems. In this group, the most important and widely used method is the enthalpy method. The advantages of the enthalpy reformulation are that the problem to be solved is formulated in a fixed region, and no modification of the numerical scheme is necessary in order to satisfy the conditions at the moving phase-change interface. Furthermore, this method is especially suitable both for the problems where the phase change occurs at a single temperature and for the problems where the phase change occurs over a temperature range.

Most of the previous enthalpy models usually treated the enthalpy as a dependent variable in addition to the temperature, and discretized the energy equation into a set of equations which contain both E and T. For the implicit schemes, they actually treated all of the terms containing $T = T(E)$ as a constant heat source term in the energy equation during iterations at each time step. This may cause some problems for convergence when $T = T(E)$ is complicated and physical properties change significantly as is the case of frozen heat pipe start-up, or when the boundary conditions are severe. Furthermore, when the energy equation contains a convective term, the previous methods have difficulties in handling the relationship between the convective and diffusive terms because of the two dependent variable nature of the equation.

NOMENCLATURE

a	coefficient
b	source term in the discretization equation
C	specific heat [J kg^{-1} K^{-1}]
D	diagonal distance [m]
E	enthalpy [J kg^{-1}]
F	flow rate through a control-volume face [kg s^{-1}]
H	latent heat [J kg^{-1}]
k	thermal conductivity [W m^{-1} K^{-1}]
L	reference length [m]
l	interface position along the diagonal [m]
Q	heat source power [W]
q	heat flux [W m^{-2}]
q_h	heat flux [W m^{-2}]
R_h	heat source radius [m]
R_0	radius of the numerical domain [m]
r	radial coordinate
St	Stefan number, $C_s(T_m-T_w)/H$ or $C_s(T_m-T_i)/H$
S	coefficient in equation (7)
s	dimensionless interface position along the diagonal, l/D
T_i	initial temperature [K]
T	temperature [K]
T_m	melting or freezing temperature [K]
T_w	wall temperature [K]
T^*	'Kirchhoff' temperature [W m^{-1}]
T_1	temperature defined in Fig. 2 [K]
T_2	temperature defined in Fig. 2 [K]
ΔT	temperature range, T_2-T_1 [K]
t	time [s]
U	heat source velocity [m s^{-1}]
u, v, w	velocities [m s^{-1}]
x, y, z	coordinate directions
Δx	x-direction width of the control volume
δx	x-direction distance between two adjacent grid points
$\Delta y, \delta y$	similar to $\Delta x, \delta x$
$\Delta z, \delta z$	similar to $\Delta x, \delta x$.

Greek symbols

α	thermal diffusivity [m^2 s^{-1}]
Γ	coefficient in equation (7)
δ	thickness [m]
η	dummy variable in equations (4) and (14)
θ	coordinate direction
θ_d	dimensionless temperature, $(T-T_m)/(T_m-T_i)$
θ_0	dimensionless temperature, $(T_i-T_w)/(T_m-T_w)$
ρ	density [kg m^{-3}]
τ	dimensionless time, $t\alpha/L^2$
ϕ	dummy variable.

Subscripts

B	'bottom' neighbor of grid P
b	control-volume face between P and B
E	'east' neighbor of grid P
e	control-volume face between P and E
i	initial condition
l	liquid phase
m	mushy phase
N	'north' neighbor of grid P
n	control-volume face between P and N
P	grid point
S	'south' neighbor of grid P
s	control-volume face between P and S or solid phase
T	'top' neighbor of grid P
t	control-volume face between P and T
W	'west' neighbor of grid P
w	control-volume face between P and W.

Some attempts have been made to overcome these difficulties [9, 10].

In this paper, a simple strategy is proposed to transform the energy equation into a non-linear equation with a single dependent variable E. Thus, solving a phase-change problem is equivalent to solving a non-linear enthalpy equation, and existing algorithms are readily applicable with some modifications.

ENTHALPY TRANSFORMATION OF THE ENERGY EQUATION

The energy equation governing three-dimensional laminar flow with no viscous dissipation and with the incorporation of the continuity equation in the Cartesian coordinate system is [11,12]

$$\frac{\partial(\rho E)}{\partial t}+\frac{\partial}{\partial x}(\rho uE)+\frac{\partial}{\partial y}(\rho vE)+\frac{\partial}{\partial z}(\rho wE)=\frac{\partial}{\partial x}\left(k\frac{\partial T}{\partial x}\right)+\frac{\partial}{\partial y}\left(k\frac{\partial T}{\partial y}\right)+\frac{\partial}{\partial z}\left(k\frac{\partial T}{\partial z}\right) \quad (1)$$

with the state equation

$$\frac{\mathrm{d}E}{\mathrm{d}T}=C(T). \quad (2)$$

In the case of constant specific heats for each phase,

and that the phase change occurs at a single temperature, we have

$$T=\begin{cases} T_m+E/C_s & E\leqslant 0 \quad \text{(solid phase)} \\ T_m, & 0<E<H \quad \text{(mushy phase)} \\ T_m+(E-H)/C_l, & E\geqslant H \quad \text{(liquid phase)} \end{cases} \tag{3}$$

where T_m is the melting or freezing temperature. In the above relation, we have selected $E=0$ to correspond to phase-change materials in their solid state at temperature T_m.

The 'Kirchhoff' temperature [13] is introduced as follows:

$$T^*=\int_{T_m}^{T} k(\eta)\,d\eta=\begin{cases} k_s(T-T_m), & T<T_m \\ 0, & T=T_m \\ k_l(T-T_m), & T>T_m. \end{cases} \tag{4}$$

Transforming equation (3) with the definition given in equation (4) results in

$$T^*=\begin{cases} k_sE/C_s, & E\leqslant 0 \\ 0, & 0<E<H \\ k_l(E-H)/C_l, & E\geqslant H \end{cases} \tag{5}$$

and equation (1) becomes

$$\frac{\partial(\rho E)}{\partial t}+\frac{\partial}{\partial x}(\rho uE)+\frac{\partial}{\partial y}(\rho vE)+\frac{\partial}{\partial z}(\rho wE) = \frac{\partial^2 T^*}{\partial x^2}+\frac{\partial^2 T^*}{\partial y^2}+\frac{\partial^2 T^*}{\partial z^2}. \tag{6}$$

Now, let us introduce an enthalpy function as follows:

$$T^*=\Gamma(E)E+S(E). \tag{7}$$

For the phase change occurring at a single temperature, we have

$$\Gamma(E)=\begin{cases} k_s/C_s, & E\leqslant 0 \\ 0, & 0<E<H \\ k_l/C_l, & E\geqslant H \end{cases} \tag{8}$$

and

$$S(E)=\begin{cases} 0, & E\leqslant 0 \\ 0, & 0<E<H \\ -Hk_l/C_l, & E\geqslant H. \end{cases} \tag{9}$$

Upon substituting equation (7) into equation (6) and noticing that, for example

$$\frac{\partial^2 T^*}{\partial x^2}=\frac{\partial}{\partial x}\left(\frac{\partial(\Gamma E+S)}{\partial x}\right)=\frac{\partial^2}{\partial x^2}(\Gamma E)+\frac{\partial^2 S}{\partial x^2}$$

we have

$$\frac{\partial(\rho E)}{\partial t}+\frac{\partial}{\partial x}(\rho uE)+\frac{\partial}{\partial y}(\rho vE)+\frac{\partial}{\partial z}(\rho wE) = \frac{\partial^2(\Gamma E)}{\partial x^2}+\frac{\partial^2(\Gamma E)}{\partial y^2}+\frac{\partial^2(\Gamma E)}{\partial z^2}+P \tag{10}$$

with

$$P=\frac{\partial^2 S}{\partial x^2}+\frac{\partial^2 S}{\partial y^2}+\frac{\partial^2 S}{\partial z^2},\quad \Gamma=\Gamma(E),\quad S=S(E).$$

The energy equation has been transformed into a nonlinear equation with a single dependent variable E. The non-linearity of the phase-change problem is evident in the above equation.

In the liquid region away from the moving front as indicated in the numerical domain of Fig. 1, equation (10) reduces to the normal linear energy equation

$$\frac{\partial(\rho_l E)}{\partial t}+\frac{\partial}{\partial x}(\rho_l uE)+\frac{\partial}{\partial y}(\rho_l vE)+\frac{\partial}{\partial z}(\rho_l wE) = \frac{\partial}{\partial x}\left(k_l\frac{\partial T}{\partial x}\right)+\frac{\partial}{\partial y}\left(k_l\frac{\partial T}{\partial y}\right)+\frac{\partial}{\partial z}\left(k_l\frac{\partial T}{\partial z}\right). \tag{11}$$

Also, in the solid region equation (10) reduces to

$$\frac{\partial(\rho_s E)}{\partial t}+\frac{\partial}{\partial x}(\rho_s uE)+\frac{\partial}{\partial y}(\rho_s vE)+\frac{\partial}{\partial z}(\rho_s wE) = \frac{\partial}{\partial x}\left(k_s\frac{\partial T}{\partial x}\right)+\frac{\partial}{\partial y}\left(k_s\frac{\partial T}{\partial y}\right)+\frac{\partial}{\partial z}\left(k_s\frac{\partial T}{\partial z}\right). \tag{12}$$

In the moving front region (the region between the two dashed lines as indicated in Fig. 1), equation (10) is nonlinear. This agrees with the well-known fact that the nonlinearity of phase-change problems is due to the existence of a moving interface [14].

The method proposed is not restricted to the forms for $\Gamma(E)$ and $S(E)$ given by equations (8) and (9). With different conditions and assumptions, they have different expressions. For example, if phase changes occur over a temperature range (such as allows), as shown in Fig. 2, with constant specific heats for each phase, we have

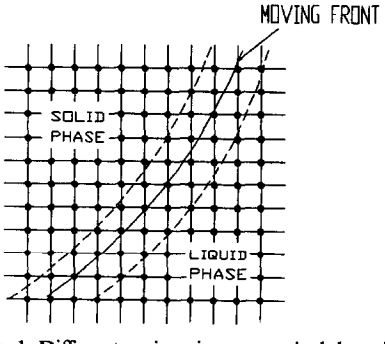

FIG. 1. Different regions in a numerical domain.

$$T-T_1=\begin{cases}E/C_s\\ \Delta TE/(H+C_m\Delta T),\\ E/C_l-[H+(C_m-C_l)\Delta T]/C_l,\end{cases}$$

$$\begin{aligned}&E\leqslant 0 && \text{(solid phase)}\\ &0<E<H+C_m\Delta T && \text{(mushy phase)}\\ &E\geqslant H+C_m\Delta T && \text{(liquid phase).}\end{aligned}\qquad(13)$$

Here, we have selected $E=0$ to correspond to phase-change materials in their solid state at temperature T_1. Then $T_m=(T_1+T_2)/2$ is defined as the melting temperature, $\Delta T=T_2-T_1$ the melting temperature range, and C_m the specific heat for the mushy phase.

The 'Kirchhoff' temperature is introduced as

$$T^*=\int_{T_1}^{T}k(\eta)\,d\eta=\begin{cases}k_s(T-T_1), & T\leqslant T_1\\ k_m(T-T_1), & T_1<T<T_2\\ k_l(T-T_1), & T\geqslant T_2\end{cases}\qquad(14)$$

where k_m is the thermal conductivity for the mushy phase. The transformation procedure is the same as that of phase change at a single temperature, and the resulting equation is still equation (10) with different expressions for $\Gamma(E)$ and $S(E)$

$$\Gamma(E)=\begin{cases}k_s/C_s, & E\leqslant 0\\ k_m\Delta T/(H+C_m\Delta T), & 0<E<H+C_m\Delta T\\ k_l/C_l, & E\geqslant H+C_m\Delta T\end{cases}\qquad(15)$$

$$S(E)=\begin{cases}0, & E\leqslant 0\\ 0, & 0<E<H+C_m\Delta T\\ -k_l[H+(C_m-C_l)\Delta T]/C_l, & E\geqslant H+C_m\Delta T.\end{cases}\qquad(16)$$

In the above relations for the mushy region, a linear change was assumed. In real systems, they may take more complicated forms. However, this is outside the scope of this paper.

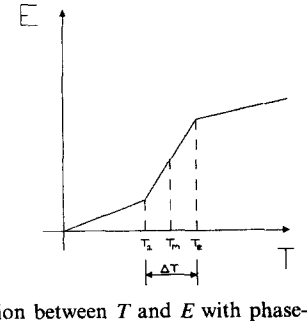

FIG. 2. Relation between T and E with phase-change temperature range.

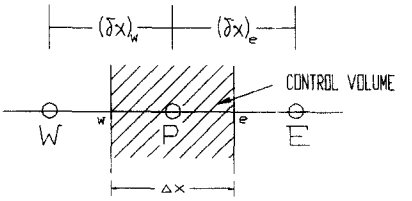

FIG. 3. Grid-point cluster for the one-dimensional problem.

NUMERICAL SCHEME

Phase change without convective terms

To demonstrate the methodology, let us consider a phase-change problem in one space dimension. In this case, equation (10) reduces to

$$\rho\frac{\partial E}{\partial t}=\frac{\partial^2}{\partial x^2}(\Gamma E)+\frac{\partial^2 S}{\partial x^2}\qquad(17)$$

with $\Gamma=\Gamma(E)$ and $S=S(E)$. The discretization of the above equation employs the control-volume finite-difference approach described by Patankar [12]. In this methodology, the discretization equations are obtained by applying conservation laws over finite size control volumes surrounding the grid nodes, and integrating the equation over the control volumes, i.e.

$$\iiint_{\Delta V}\rho\frac{\partial E}{\partial t}\,dV=\iiint_{\Delta V}\left(\frac{\partial^2(\Gamma E)}{\partial x^2}+\frac{\partial^2 S}{\partial x^2}\right)dV.\qquad(18)$$

Using a fully implicit scheme and referring to Fig. 3, we have

$$\iiint_{\Delta V}\frac{\partial E}{\partial t}\,dV=\rho\Delta x\frac{E_P-E_P^0}{\Delta t}\qquad(19)$$

$$\iiint_{\Delta V}\frac{\partial^2}{\partial x^2}(\Gamma E)\,dV=\left(\frac{\partial(\Gamma E)}{\partial x}\right)_e-\left(\frac{\partial(\Gamma E)}{\partial x}\right)_w=\frac{\Gamma_E E_E-\Gamma_P E_P}{(\delta x)_e}-\frac{\Gamma_P E_P-\Gamma_W E_W}{(\delta x)_w}\qquad(20)$$

$$\iiint_{\Delta V}\frac{\partial^2 S}{\partial x^2}\,dV=\frac{S_E-S_P}{(\delta x)_e}-\frac{S_P-S_W}{(\delta x)_w}.\qquad(21)$$

Thus

$$a_P E_P=a_E E_E+a_W E_W+b\qquad(22)$$

with E_P^0 denoting the old value of E at grid point P

$$a_E=\frac{\Gamma_E}{(\delta x)_e},\quad a_W=\frac{\Gamma_W}{(\delta x)_w}$$

$$b=\frac{\rho\Delta x E_P^0}{\Delta t}+\frac{S_E-S_P}{(\delta x)_e}-\frac{S_P-S_W}{(\delta x)_w}$$

and

$$a_P = \frac{\Gamma_P}{(\delta x)_e} + \frac{\Gamma_P}{(\delta x)_w} + \frac{\rho \Delta x}{\Delta t}.$$

Phase change with a convective term

In this case, a one space dimensional problem will also be considered as a demonstrative example. The governing equation is

$$\frac{\partial(\rho E)}{\partial t} + \frac{\partial}{\partial x}(\rho u E) = \frac{\partial^2}{\partial x^2}(\Gamma E) + \frac{\partial^2 S}{\partial x^2}. \quad (23)$$

Since the total flux in the above equation

$$J = \rho u E - \frac{\partial}{\partial x}(\Gamma E)$$

is different from the conventional total flux

$$J = \rho u \phi - \Gamma \frac{\partial \phi}{\partial x}$$

the usual method to obtain the convection–diffusion expression is not applicable. Also, the coefficient Γ is small in most cases. In order to handle convection–diffusion situations and ensure physically realistic solutions, a scheme similar to the upwind scheme is employed. The discretization equation is written as

$$a_P E_P = a_E E_E + a_W E_W + b \quad (24)$$

where

$$a_P = a_{PE} + a_{PW} + \frac{\Delta x}{\Delta t}\rho_P^0$$

$$a_E = \Gamma_E D_e + \max[-F_e, 0]$$

$$a_{PE} = \Gamma_P D_e + \max[-F_e, 0]$$

$$a_W = \Gamma_W D_w + \max[F_w, 0]$$

$$a_{PW} = \Gamma_P D_w + \max[F_w, 0]$$

$$b = \frac{\rho_P^0 \Delta x E_P^0}{\Delta t} + \frac{S_E - S_P}{(\delta x)_e} - \frac{S_P - S_W}{(\delta x)_w}$$

$$D_e = 1/(\delta x)_e, \quad F_e = (\rho u)_e$$

$$D_w = 1/(\delta x)_w, \quad F_w = (\rho u)_w.$$

The greater of a and b is given by max $[a, b]$, E_P^0 denotes the old value of E at grid point P, and ρ_P^0 denotes the old value of ρ at grid point P. The subscripts E and e for example, denote the values at grid E and control-volume face e, respectively, for Γ, S, F and D. It is clear that no special treatment is needed for solving the velocity using momentum equations.

Phase change for multi-dimensional problems

Having described the discretization equation for one space dimensional problems, we can now write a discretization based on the general differential equation (10) for multi-dimensional problems, with E, W, N, S, T, and B representing the 'east', 'west', 'north', 'south', 'top', and 'bottom' neighbors of node P, respectively. The corresponding discretization equation is

$$a_P E_P = a_E E_E + a_W E_W + a_N E_N + a_S E_S + a_T E_T + a_B E_B + b \quad (25)$$

where

$$a_P = a_{PE} + a_{PW} + a_{PN} + a_{PS} + a_{PB} + a_{PT} + \frac{\Delta x \Delta y \Delta z \rho_P^0}{\Delta t}$$

$$a_E = \Gamma_E D_e + \max[-F_e, 0], \quad a_{PE} = \Gamma_P D_e + \max[-F_e, 0]$$

$$a_W = \Gamma_W D_w + \max[F_w, 0], \quad a_{PW} = \Gamma_P D_w + \max[F_w, 0]$$

$$a_N = \Gamma_N D_n + \max[-F_n, 0], \quad a_{PN} = \Gamma_P D_n + \max[-F_n, 0]$$

$$a_S = \Gamma_S D_s + \max[F_s, 0], \quad a_{PS} = \Gamma_P D_s + \max[F_s, 0]$$

$$a_T = \Gamma_T D_t + \max[-F_t, 0], \quad a_{PT} = \Gamma_P D_t + \max[-F_t, 0]$$

$$a_B = \Gamma_B D_b + \max[F_b, 0], \quad a_{PB} = \Gamma_P D_b + \max[F_b, 0]$$

$$b = \frac{\Delta x \Delta y \Delta z \rho_P^0}{\Delta t} E_P^0 + D_e(S_E - S_P) - D_w(S_P - S_W) + D_n(S_N - S_P) - D_s(S_P - S_S) + D_t(S_T - S_P) - D_b(S_P - S_B).$$

The flow rates and conductances are defined as

$$F_e = (\rho u)_e \Delta y \Delta z, \quad D_e = \frac{\Delta y \Delta z}{(\delta x)_e}$$

$$F_w = (\rho u)_w \Delta y \Delta z, \quad D_w = \frac{\Delta y \Delta z}{(\delta x)_w}$$

$$F_n = (\rho v)_n \Delta z \Delta x, \quad D_n = \frac{\Delta z \Delta x}{(\delta y)_n}$$

$$F_s = (\rho v)_s \Delta z \Delta x, \quad D_s = \frac{\Delta z \Delta x}{(\delta y)_s}$$

$$F_t = (\rho w)_t \Delta x \Delta y, \quad D_t = \frac{\Delta x \Delta y}{(\delta z)_t}$$

$$F_b = (\rho w)_b \Delta x \Delta y, \quad D_b = \frac{\Delta x \Delta y}{(\delta z)_b}. \quad (26)$$

Because of the nonlinearity of the above equation and the implicit nature of the scheme, iterations are needed at each time step. This procedure is the same as that which solves a non-linear equation, and is given below.

(1) Let E^k represent the E field as it exists at the beginning of the kth iteration.

(2) From these values, calculate tentative values of Γ and S according to their relations with E, using equations (8) and (9), or equations (15) and (16).

(3) Solve the nominally linear set of discretization equations to get new values of E^{k+1}.

(4) Return to step 1 and repeat the process until further iterations cease to produce any significant change in the values of E.

APPLICATION OF THE METHODOLOGY TO THE EXAMPLE PROBLEMS

To demonstrate the present scheme, the proposed methodology has been applied to two separate phase-

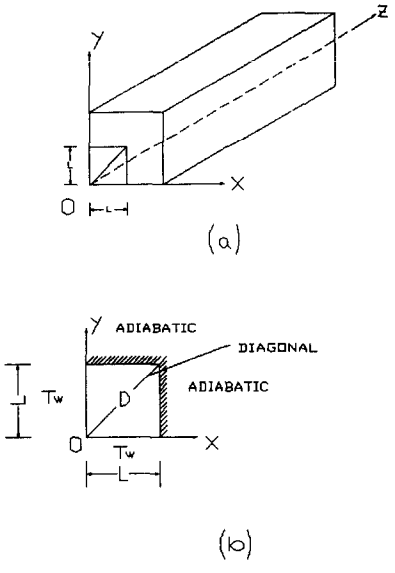

FIG. 4. Description of the geometry and boundary conditions for the three-dimensional freezing problem. (a) Bar of liquid with a uniform square cross section. (b) One-quarter of the bar used for the computational domain due to the symmetry of the problem.

change problems. The first is a three-dimensional freezing problem, and the second is a three-dimensional moving heat source problem. In the two problems considered herein, the thermal physical properties such as k and C are assumed to be constant in each phase but may differ among the solid, mushy and liquid phases, while the density ρ is considered the same for each phase.

The three-dimensional freezing problem

Consider a liquid initially at its melting temperature T_m in a bar with a uniform square cross-section and adiabatic ends as shown in Fig. 4(a). The surface is suddenly exposed to a uniform wall temperature below the fusion temperature and freezing takes place immediately. Because of the symmetry of the geometry, only a quarter of the bar is considered as shown in Fig. 4(b). To facilitate comparison, the dimensionless parameters are chosen to be the same as those used by Hsiao and Chung [6], i.e.

$$\theta_0 = (T_i - T_w)/(T_m - T_w) = 1$$

and

$$St = C_s(T_m - T_w)/H = 0.641.$$

At the middle plane of the bar in the z-direction, the temperature distribution is two-dimensional. Figure 5 shows the interface position as a function of time along the diagonal for the present three-dimensional modeling. The two-dimensional results given by Hsiao and Chung [6] using the equivalent heat capacity model and given by Crowley [4] using the enthalpy model are also included in the same figure. As can be seen, the agreement among these solutions is excellent.

Consider the same problem with different initial conditions and physical properties ($T_i > T_m$). The dimensionless parameters are $k_l/k_s = 0.9$, $\alpha_l/\alpha_s = 0.9$, $\theta_0 = (T_i - T_w)/(T_m - T_w) = 9/7$ and $St = C_s(T_m - T_w)/H = 2$. Figure 6 shows the interface position as a function of time along the diagonal. Also included in Fig. 6 are solutions obtained by Hsiao and Chung [6], and by Keung [7]. Again, the present three-dimensional solution agrees well with the results of those two-dimensional studies.

The above calculation is based on the fact that the phase change occurs at a single temperature. Assuming that the phase change takes place over a temperature range of $\Delta T = 20$ K, the same calculation is conducted, and the results are also presented in Fig.

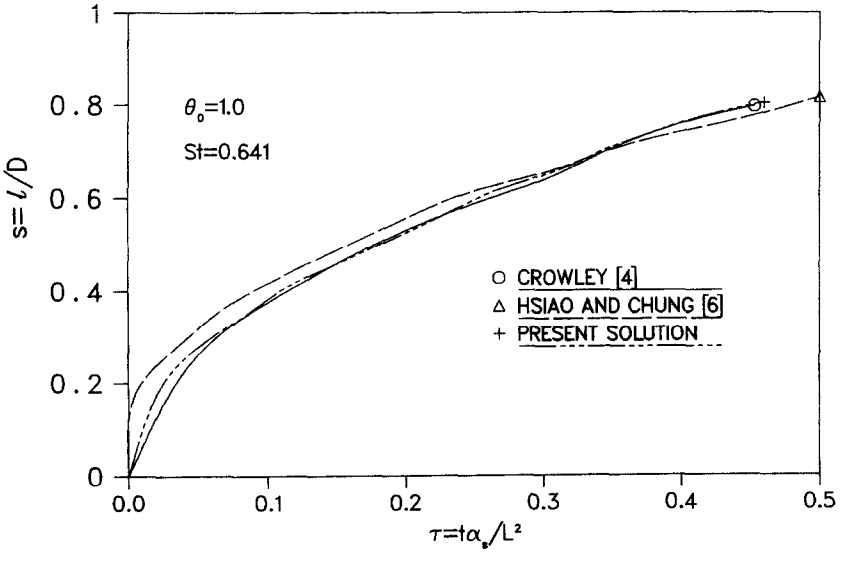

FIG. 5. Interface position along the diagonal for solidification of a saturated liquid.

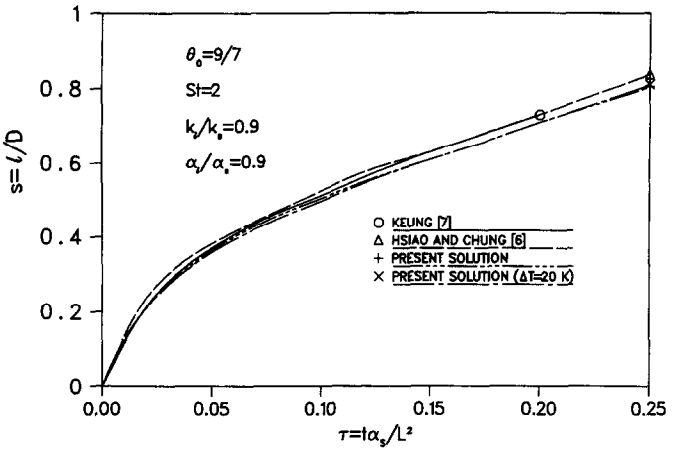

FIG. 6. Interface position along the diagonal with prescribed boundary temperature.

6. It can be seen that the present model is insensitive to the phase-change temperature range. If the temperature range is small enough, the same result as that of the single temperature case is expected. This is the case for the present model. The calculation is conducted with $\Delta T = 2$ K, and the result is almost identical to that of the single temperature case in Fig. 6.

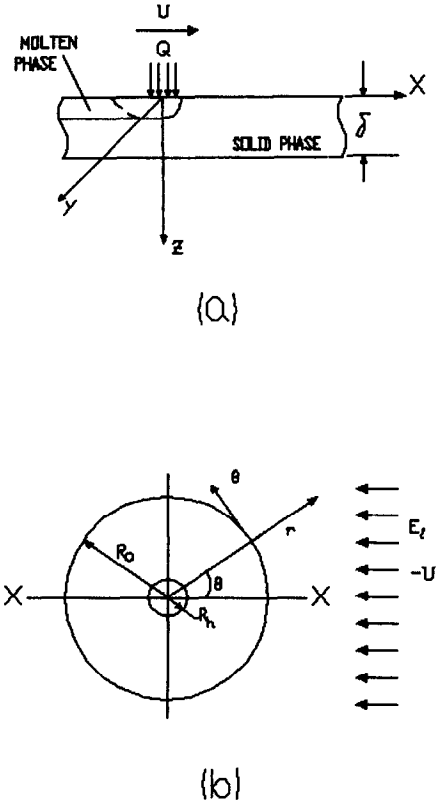

FIG. 7. Pictorial description of moving heat source problem. (a) Side-view of the computational domain with the heat source moving at speed U. (b) Top-view of the computational domain with the heat source stationary and the computational domain moving at speed $-U$.

The accuracy of the numerical solution was checked by varying the grid spacing systematically. The final grid size employed in the above two cases is $20 \times 20 \times 30$ and the discretization equations are solved by the Gauss–Seidel method. The physical properties of the mushy phase are taken as the average of those of the solid and liquid phases. The time step limit is not encountered in the calculations. The dimensionless time steps can be of the order of 0.1, and real time steps can be as large as several days.

Three-dimensional phase-change problem with moving heat source

As indicated in Fig. 7, a source of heat moves over the surface of the plate with speed U. Due to intense heating, the material under the heat source melts. It is important to determine the molten depth for the given velocity, heat source power and its diameter, as well as the material properties.

With the coordinates fixed at the center of the moving heat source, equation (10) is applicable for this problem. In order to simulate the circular heat source, the equation has been transformed into the form for the cylindrical–polar coordinate system.

The governing equation is

$$\frac{\partial(E\rho)}{\partial t} + \frac{1}{r}\frac{\partial(rv_r\rho E)}{\partial r} + \frac{1}{r}\frac{\partial(v_\theta \rho E)}{\partial \theta} = \frac{1}{r}\frac{\partial}{\partial r}\left[r\frac{\partial(\Gamma E)}{\partial r}\right] + \frac{1}{r}\frac{\partial}{\partial \theta}\left[\frac{1}{r}\frac{\partial(\Gamma E)}{\partial \theta}\right] + \frac{\partial}{\partial z}\left[\frac{\partial(\Gamma E)}{\partial z}\right] + P \quad (27)$$

where

$$P = \frac{1}{r}\frac{\partial}{\partial r}\left[r\frac{\partial S}{\partial r}\right] + \frac{1}{r}\frac{\partial}{\partial \theta}\left[\frac{1}{r}\frac{\partial S}{\partial \theta}\right] + \frac{\partial^2 S}{\partial z^2}$$

$$v_r = -U\cos\theta, \quad v_\theta = U\sin\theta$$

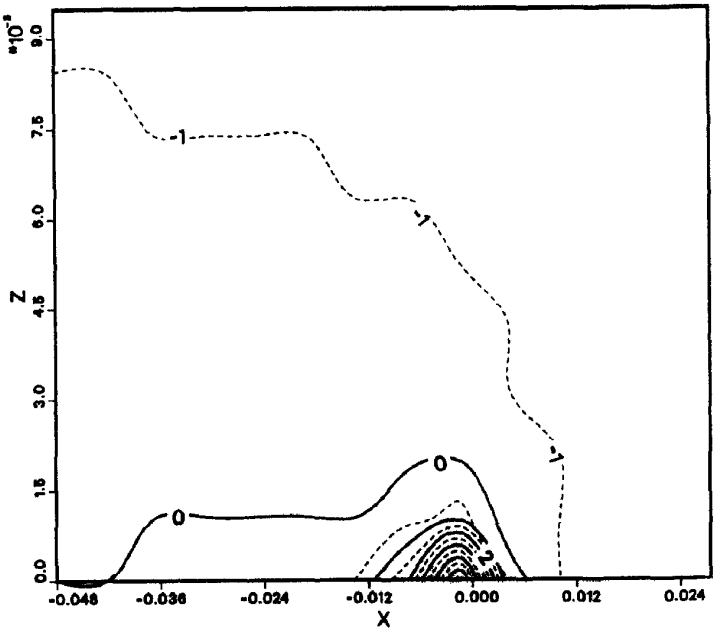

FIG. 8. Isotherms of the solutions for $t = 0.1$ s at the X–X plane.

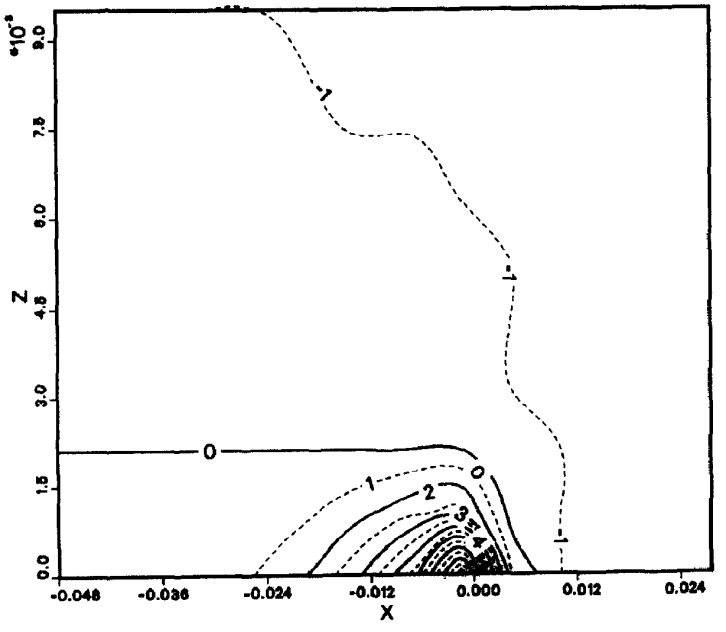

FIG. 9. Steady-state isotherms of the solution at the X–X plane.

and

$$\Gamma = \Gamma(E),\ S = S(E)$$

are given by equations (8) and (9), respectively. The initial and boundary conditions are as follows:

$$E_i = C_s(T_i - T_m) \quad t = 0$$

$$t > 0$$

$$q = q_h \qquad z = 0,\quad r \leqslant R_h$$

$$q = 0 \qquad z = 0,\quad r > R_h$$

$$q = 0 \qquad z = \delta$$

$$E = E_i \qquad r = R_0,\quad -90° \leqslant \theta \leqslant 90°$$

$$\frac{\partial(\Gamma E + S)}{\partial r} = 0 \quad r = R_0,\quad 90° < \theta < 270°.$$

The radius R_0 must be sufficiently large such that the region $r \geqslant R_0$, $-90° \leqslant \theta \leqslant 90°$ is unaffected by the moving heat source. Also, the last boundary condition implies that the upwind scheme is used and the diffusive term is neglected for the outflow boundary. The calculation proceeds with grid size $32 \times 50 \times 12$ and time step 0.1 s. Other parameters are

$$U = 0.3\,\mathrm{m\,s^{-1}},\quad \alpha_s/\alpha_l = 1.44$$

$$St = C_s(T_m - T_i)/H = 0.126$$

$$R_h = 0.005\,\mathrm{m},\quad R_0 = 0.25\,\mathrm{m},\quad Q = 11.80\,\mathrm{kW}.$$

Figure 8 shows isotherms of the dimensionless temperature $\theta_d = (T - T_m)/(T_m - T_i)$ for $t = 0.1$ s at the X–X plane indicated in Fig. 7(b) (i.e., $\theta = 0°$ and 180°). The center of the heat source is located at $x = 0$. The solid line labelled 0 indicates the melting front at this time, while the dashed line labelled -1 is a boundary beyond which the temperature field is unaffected by the moving heat source. After about 0.5 s, the steady-state condition is reached. Figure 9 shows the steady-state isotherms of the dimensionless temperature at the same plane. As can be seen, the melting front line becomes flat in the portion of $x < 0$.

CONCLUSIONS

The enthalpy transforming model proposed in this paper proves to be capable of handling complicated phase-change problems occurring both at a single temperature and a temperature range with fixed grids. Due to the one dependent variable nature of the transformed equation, the convection and diffusion situations can be handled with appropriate algorithms. Comparisons have been made with the numerical results existing in the literature with a good agreement, showing that the present model can properly predict the phase-change processes. The advantage of this model based on enthalpy is that it allows us to avoid paying explicit attention to the nature of the phase-change front, and can be extended to complicated multi-dimensional problems with convective terms without involving cumbersome mathematical schemes.

Acknowledgement—Funding for this work was provided by a NASA–Air Force joint effort under contract F-33615-88-C-2820.

REFERENCES

1. M. Okada, Analysis of heat transfer during melting from a vertical wall, *Int. J. Heat Mass Transfer* **27**, 2057–2066 (1984).
2. C. J. Ho and S. Chen, Numerical simulation of melting of ice around a horizontal cylinder, *Int. J. Heat Mass Transfer* **29**, 1359–1368 (1986).
3. N. Shamsunder and E. M. Sparrow, Analysis of multi-dimensional conduction phase-change via the enthalpy model, *ASME J. Heat Transfer* **97**(3), 333–340 (1975).
4. A. B. Crowley, Numerical solution of Stefan problems, *Int. J. Heat Mass Transfer* **21**, 215–218 (1978).
5. V. R. Voller and M. Cross, Estimating the solidification/melting times of cylindrically symmetric regions, *Int. J. Heat Mass Transfer* **24**, 1457–1462 (1981).
6. J. S. Hsiao and B. T. F. Chung, An efficient algorithm for finite element solution to two-dimensional heat transfer with melting and freezing, ASME Paper No. 84-HT-2 (1984).
7. C. S. Keung, The use of sources and sinks in solving two-dimensional heat conduction problems with change of phase in arbitrary domains, Ph.D. Dissertation, Columbia University (1980).
8. J. S. Hsiao, An efficient algorithm for finite difference analysis of heat transfer with melting and solidification, ASME Paper No. 84-WA/HT-42 (1984).
9. V. R. Voller and C. Prakash, A fixed grid numerical modelling methodology for convection–diffusion mushy region phase-change problems, *Int. J. Heat Mass Transfer* **30**, 1709–1718 (1987).
10. W. D. Bennon and F. P. Incropera, A continuum model for momentum, heat and species transport in binary solid–liquid phase change systems—I. Model formulation, *Int. J. Heat Mass Transfer* **30**, 2161–2170 (1987).
11. W. M. Kays and M. E. Crawford, *Convective Heat and Mass Transfer* (2nd Edn). McGraw-Hill, New York (1980).
12. S. V. Patankar, *Numerical Heat Transfer and Fluid Flow*. McGraw-Hill, New York (1980).
13. A. D. Solomon, M. D. Morris, J. Martin and M. Olszewski, The development of a simulation code for a latent heat thermal energy storage system in a space station, Technical Report ORNL-6213 (1986).
14. M. N. Ozisik, *Heat Conduction*. Wiley, New York (1980).

ANALYSE NUMERIQUE DES PROBLEMES DE STEFAN POUR DES STRUCTURES A CHANGEMENT DE PHASE TRIDIMENSIONNELLES, A PARTIR DU MODELE DE TRANSFORMATION ENTHALPIQUE

Résumé—On propose un schéma de transformation enthalpique pour convertir l'équation d'énergie en une équation non linaire dans laquelle l'enthalpie E est l'unique variable. L'approche par différence entre volumes finis de contrôle est modifiée pour être appliquée aux problèmes de Stefan. Le modèle est testé en l'appliquant à un problème trimensionnel de gel. Les résultats numériques s'accordent avec ceux de la bibliographie. Le modèle et son algorithme sont ensuite appliqués à un problème tridimensionnel de source de chaleur mobile qui montre que la méthodologie est capable de traiter des problèmes de changement de phase avec des grilles fixes.

NUMERISCHE UNTERSUCHUNG VON STEFAN-PROBLEMEN FÜR VERALLGEMEINERTE MEHRDIMENSIONALE PHASENWECHSELSTRUKTUREN MIT HILFE DER ENTHALPHIEMETHODE

Zusammenfassung—Ein Transformationsschema soll die Energiegleichung in eine nichtlineare Gleichung mit der Enthalpie E als einziger abhängiger Variablen umwandeln. Mit Hilfe eines modifizierten Finite-Differenzen-Verfahrens kann dann das Stefan-Problem gelöst werden. Das Modell wird durch Anwendung auf ein dreidimensionales Gefrierproblem überprüft. Die numerischen Ergebnisse stimmen dabei mit Literaturwerten überein. Außerdem wird das Modell auf ein dreidimensionales Problem mit beweglicher Wärmequelle angewandt um zu zeigen, daß die Methode für komplizierte Phasenwechselprobleme mit fester Gitterteilung geeignet ist.

ЧИСЛЕННЫЙ АНАЛИЗ ЗАДАЧ СТЕФАНА ДЛЯ ОБОБЩЕННЫХ МНОГОМЕРНЫХ СТРУКТУР С ФАЗОВЫМ ПЕРЕХОДОМ ПРИ ИСПОЛЬЗОВАНИИ МОДЕЛИ ПРЕОБРАЗОВАНИЯ ЭНТАЛЬПИИ

Аннотация—Предложена схема, использующая преобразование энтальпии для получения нелинейного уравнения сохранения энергии, в котором энтальпия E является единственной зависимой переменной. Существующий конечно-разностный метод контрольного объема модифицируется в применении к численным решениям задач Стефана. Модель проверена на трехмерной задаче замораживания. Численные результаты хорошо согласуются с имеющимися в литературе данными. Далее модель и ее алгоритм применяются к трехмерной задаче для движущегося источника тепла, и показано, что данная методология может успешно использоваться для решения сложных задач фазового перехода с заданными сетками.